Gene Expression in Retinal Ischemic Post-conditioning

Konrad Kadzielawa, B.S.[1], **Biji Mathew, Ph.D.**[1], **Clara R. Stelman, B.S.**[1], **Arden Zhengdeng Lei, Ph.D.**[3], **Leianne Torres, M.D.**[1], and **Steven Roth, M.D.**[1,2]

[1]Department of Anesthesiology, University of Illinois at Chicago, Chicago, IL, USA

[2]Department of Ophthalmology, University of Illinois at Chicago, Chicago, IL, USA

[3]Center for Research Bioinformatics, University of Illinois at Chicago, Chicago, IL, USA

Abstract

Purpose—The pathophysiology of retinal ischemia involves mechanisms including inflammation and apoptosis. Ischemic post-conditioning (Post-C), a brief non-lethal ischemia, induces a long-term ischemic tolerance, but the mechanisms of ischemic post-conditioning in the retina have only been described on a limited basis. Accordingly, we conducted this study to determine the molecular events in retinal ischemic postconditioning and to identify targets for therapeutic strategies for retinal ischemia.

Methods—To determine global molecular events in ischemic Post-Conditioning, a comprehensive study of the transcriptome of whole retina was performed. We utilized RNA-Sequencing (RNA-Seq), a recently developed, deep sequencing technique enabling quantitative gene expression, with low background noise, dynamic detection range, and discovery of novel genes. Rat retina was subjected to ischemia *in vivo* by elevation of intraocular pressure above systolic blood pressure. At 24 h after ischemia, Post-C or sham Post-C was performed by another, briefer period of ischemia, and 24 h later, retinas were collected and RNA processed.

Results—There were 71 significantly affected pathways in post-conditioned/ischemic *vs* normals and 43 in sham post conditioned/ischemic *vs* normal. Of these, 28 were unique to Post C and ischemia. Seven biological pathways relevant to ischemic injury, in Post-C as opposed to sham Post C, were examined in detail. Apoptosis, p53, cell cycle, Jak-Stat, HIF-1, MAPK and PI3K-Akt pathways significantly differed in the number as well as degree of fold change in genes between conditions.

Conclusion—Post-C is a complex molecular signaling process with a multitude of altered molecular pathways. We identified potential gene candidates in Post-C. Studying the impact of altering expression of these factors may yield insight into new methods for treating or preventing damage from retinal ischemic disorders.

Address correspondence to: Steven Roth, M.D., Department of Anesthesiology, MC 515, University of Illinois Medical Center, 1740 West Taylor Street, Chicago, Illinois 60612 USA, rothgas@uic.edu, 312-996-0052 (telephone), 773-753-1024 (fax).

Keywords

ischemia; post-conditioning; retina; RNA-Seq

INTRODUCTION

Central retinal artery occlusion (CRAO) due to thrombus or embolism, occurring at an incidence of 1–15/10,000 yearly, develops into retinal ischemia, often impairing visual acuity to < 20/400. Severe visual loss increases healthcare costs, mortality and depression; and decreases productivity, independence, and quality of life. Retinal ischemia is also, significantly, a final common pathway in major, chronic vision-threatening diseases including retinal vein occlusion and diabetic retinopathy (DR), and may also be related to the development of age-related maculopathy (ARM). Rodent models of ischemia-reperfusion produce an injury resembling DR. [1] In chronic disease such as DR, there are few available effective treatments. While we, and, subsequently, others, have shown that the retina possesses a potent, endogenous neuroprotective capacity [2, 3], potentially accessible for clinical therapy, application to patients with DR at risk to develop DR has not yet been realized [4]. An obstacle to progress has been the incomplete understanding of retinal ischemia mechanisms and how to safely, efficiently, and precisely access therapeutic molecular targets. We previously demonstrated some of the novel mechanisms of the retina's endogenous neuroprotective capacity. Ischemic tolerance is amongst the most promising modulators of ischemic injury shown to date because it can harness endogenous mechanisms to improve recovery even as late as 24-h after an ischemic event, a mechanism known as post-conditioning (or Post-C) [2].

Post conditioning is a brief period of ischemia applied to the retina after the damaging ischemia. It has also been shown to provide neuroprotection in stroke models in brain and in cardioprotection after myocardial ischemia. [5, 6] Some of the underlying mechanisms in Post-C have been described. Post-C attenuated apoptotic cell death [2]. Also, Post-C required activation of Akt, tied to numerous downstream cell survival mediators [7]. It is likely that multiple signaling pathways and altered gene expression are involved in the neuroprotective mechanism of Post-C. In order to identify changes in global gene expression a comprehensive approach is necessary. Accordingly, the goal of the present study was an in-depth analysis of the global molecular mechanisms by which Post-C produces its neuroprotective function.

Comprehensive analysis of the transcriptome is one of the most useful approaches in understanding global molecular events, with two main techniques based largely on hybridization or sequencing [8]. Hybridization, i.e. microarrays, is well-established and remains popular mostly due to its low-cost. Nevertheless, microarrays suffer from many limitations, e.g., their reliance upon existing knowledge about genome sequence; high background levels owing to cross-hybridization; and a limited dynamic range of detection owing to both background and saturation of signals. Moreover, comparing expression levels across different experiments is difficult and can require complicated normalization methods [9]. RNA sequencing (RNA-Seq) is a relatively new technique using a sequencing–based

approach to enable global and quantitative examination of the entire transcriptome. It offers two key benefits over the microarray method: it is not limited to detecting transcripts corresponding to existing genomic sequences, and it has very low background signal because DNA sequences are unambiguously mapped to unique regions of the genome [9]. Accordingly, in this study, we used RNA-Seq to study the global gene expression changes in rat retina *in vivo* subjected to ischemia and Post-C. The goals were to define the changes in gene expression resulting from Post-C and to thus comprehensively describe molecular mechanisms of Post-C in the retina.

MATERIALS & METHODS

Animals

Procedures were approved by our institutional Animal Care Committee. Male Wistar rats (200–250 gm, Harlan, Indianapolis, IN, USA) were maintained on a 12 h on/12 h off light cycle. Experiments were performed during daylight hours. Eyes were treated with topical vigamox and cyclomydril, and for local anesthesia for needle placement, 0.5% proparacaine. For retinal ischemia, rats were anesthetized with ketamine 100 mg/kg and xylazine 7 mg/kg i.p. After sterile preparation, and working under an operating microscope, a 30-gauge, 5/8-inch metal needle (BD Precision Glide; Becton-Dickinson, Franklin Lakes, NJ, USA) was placed with its tip directed away from the lens, just inside the anterior chamber of the right eye, the experimental eye, while the left eye was control eye. To enable pressurization for increasing intraocular pressure (IOP), and measuring IOP, the needle was connected by a length of plastic tubing via a three-way stopcock to an electronic pressure transducer (Transpac 42661-04-27; Abbott, North Chicago, IL, USA) and to an elevated bag of balanced salt solution (BSS; by sterile technique, BSS was transferred from its bottle to an empty 1000-mL 0.9% saline plastic bag [Baxter, Deerfield, IL, USA]). IOP, continually displayed on a monitor (Hewlett-Packard HP78534C; Palo Alto, CA, USA), was increased to 130–135 mmHg and maintained constantly for 55 minutes by pressurizing the bag (Smiths Medical Clear-Cuff, Dublin, OH, USA). The temperature was maintained at 36–37 °C with a servo–controlled heating blanket (Harvard Apparatus, Natick, MA, USA). Oxygen saturation was measured by pulse oximetry (Ohmeda; Louisville, CO, USA) with a Band-Aid type probe on the tail. Supplemental oxygen, when necessary to maintain O_2 saturation > 93%, was administered using a cannula in front of the nares and mouth. For the Post-C stimulus, the same procedure was used to increase IOP for 5 min; Post-C or sham Post-C was done 24 h after ischemia, and eyes were collected 24 h after Post-C or sham Post-C.

After euthanasia, eyes were removed and whole retinal homogenates were prepared. Thus a mixture of retinal cell types was analyzed and results must be interpreted in light of this limitation vs single cell analysis. Four biological groups, each with 4 replicates were used in the analysis: retina control (**ShamN**), retina + postconditioning (**PCN**), retina + ischemia + sham Post-C (**ShamI**), and retina + ischemia + Post-C (**PCI**). Four pairwise comparisons between groups were generated by the Fisher's exact test: PCI *vs* ShamI, ShamI *vs* ShamN, PCI *vs* ShamN and PCN *vs* ShamN each yielding a separate table of fold changes, $\log_2$(counts per million), P and Q values. In order to examine the Post-C key regulator gene

functions and locations within the molecular pathways, as well as the impact of Post-C on gene expression after ischemia, we performed a downstream functional and pathway analysis separately for each of our biological groups, i.e., the effects of Post-C on ischemia were derived by contrasting the individual differences between PCI *vs* ShamN and ShamI *vs* ShamN.

RNA Isolation and Library Preparation

Total RNA was extracted from frozen retinal tissue, homogenized using TRIzol (Invitrogen, Carlsbad, CA, USA) and Direct-Zol RNA microPrep (Zymo Research, Irvine, CA, USA) according to the manufacturer's protocols. To purify the RNA, the homogenate was passed through Zymo-Spin columns (Zymo Research, Irvine, CA, USA). RNA quality and purity was assessed using the Agilent 2200 TapeStation (Wilmette, IL), Qubit 3.0 Fluorometer (Life Technologies, Grand Island, NY, USA), and Nanodrop. 260/280 ratios were measured for all RNA samples, with a range of 1.8–2.4. Most samples had a 260/280 ratio of 2–2.1. RNA-Seq libraries were prepared using the QuantSeq 3′ mRNA sequencing library preparation kit for Illumina sequencing platform-compatible libraries (Lexogen, Greenland, NH), according to the manufacturer's instructions. The QuantSeq protocol (seq: https://www.lexogen.com/quantseq-3mrna-sequencing/) only requires single direction sequencing. This is because only the region adjacent to the poly(A) tail of mRNAs is sequencing, and the sequencing reaction heads towards the poly(A) tail. If the reverse read were implemented, only a poly(A) sequence would be recovered. Non-coding sequences are not detected using these methods.

50 ng of total RNA were used as input template, and 18 amplification cycles were performed. The amplification step is an essential part of the RNAseq library preparation protocol. This step has three purposes, including: (a) increase of total concentration of molecules via PCR to generate sufficient material for the sequencer, (b) incorporation of sample-specific barcode sequences into the final molecules, and (c) incorporation of Illumina sequencing adapters into the final molecules. The PCR step is part of the manufacturer's instructions. Final libraries for each sample were quantified using quantitative PCR (Real-time PCR library amplification Kit; Kapa Biosystems, Boston, MA, USA). During preparation of the messenger RNAs for sequencing, a unique artificial sequence (barcode) is incorporated during the PCR amplification step. Since every molecule in a sample is labeled with the same barcode, samples from multiple samples can be pooled before sequencing. This approach is used because there is no easy way to physically separate samples on a sequencing flow cell, and because a single flow cell produces much more data than is needed for each sample. The combined library pool was sequenced using an Illumina Nextseq500 sequencer (Illumina, San Diego, CA, USA), employing a high-output kit with 80 base single-end reads. Libraries were prepared in the UIC Core Genomics Facility (CGF) and sequencing was performed in the DNA Services Facility (DNASF).

RNA-Seq Analysis

A) Count Matrix Preparation—First, we assessed the sequencing quality of raw reads with FastQC, which in contrast to quality control (QC) reports generated by the sequencer itself, detects problems which originate either in the sequencer or in the starting library

material [10]. The raw sequence reads were aligned to the reference (rat) genome using the Burrows-Wheeler Aligner (BWA-MEM), an algorithm aligning long sequences < 1 Mb size against a large sequence database (e.g., human genome). This process efficiently maps reads with read-through into polyA tails and adapter sequences, as is common with 3′ RNA-Seq [11]. To quantitate the expression levels, we used featureCounts, a program that uses a highly efficient, general-purpose read summarization to approximate counts for genomic features including genes, exons, promoter, gene bodies, genomic bins and chromosomal locations [12]. The output, i.e., the table of raw counts, was used for the following analyses.

B) Data Exploration and Quality Assessment—Raw counts were generated for 17,311 genes across 16 samples (4 biological replicates in 4 groups). To demonstrate the structure of the data, Supp. Table 1 displays the first 20 rows of raw count data. For complete raw count data, see Supplemental Table 1, or the weblink: https://uofi.box.com/s/7cpuceq42fz0tk6jpgp8e9cvl9fiv2in. For preliminary quality assessment, genes with very low counts across all samples were first filtered using the cpm (counts per million) function in edgeR for cpm> 1 in at least 4 samples [13, 14]. Subsequently, to account for the RNA composition effect, i.e., highly expressed genes consuming a substantial proportion of the total library size, resulting in under-sampling of the remaining genes, Trimmed Mean Values (TMM) normalization was performed [13]. Results were then normalized with respect to library size (reads/million) using edgeR's cpm function [13, 14]. A prior count of 2 was added to avoid logarithm evaluation errors and values were $\log_2$-transformed in order to make the counts approximately homoskedastic i.e. similar error variances across samples.

C) Differential Expression Analysis—The differential expression statistics of the data were also compiled using edgeR [14]. With the filtered raw count values as input, a negative binomial model was fitted, common dispersion estimates for each gene were obtained and Fisher's exact test was performed for each of our pre-defined pairwise comparisons [14]. Genes were considered significantly up-regulated if $\log_2$(fold change) 1and False Discovery Rate-adjusted p value (FDR) 0.05 with Benjamin and Hochberg correction for multiple tests [15] (FDR will also sometimes be referred here as a Q value). Genes were considered significantly down-regulated with $\log_2$(fold change) −1 and Q 0.05.

D) Functional Enrichment Analysis in Ischemia and Post-conditioning—
Functional enrichment analysis was performed on differentially expressed genes (absolute value of fold change 1 and Q 0.05) in each group using FunRich, a stand-alone software tool for functional enrichment and interaction network analysis [16] using the Gene Ontology rat database (Taxon ID: 10116) [17, 18]. FunRich was used due to its intuitive layout, built-in graphical tools that were publication quality as well as the ability to completely customize the background databases against which the gene sets were run. The functional enrichment tool DAVID is severely limited both in graphical outputs and the annotation databases are frequently outdated. Regulation of biological processes and molecular functions was considered significant when P 0.05, and "unique" if a given function's P value was 0.05 in one group and > 0.05 in the comparison group. To illustrate, "Apoptotic Process" had P < 0.001 associated with PCI *vs* ShamN and P=0.12 associated with ShamI *vs* ShamN; hence "Apoptotic Process" was considered a uniquely affected

process in PCI *vs* ShamN. The results of the functional enrichment analysis were used for inference of the gene pathways affected.

E) Pathway/Impact Analysis of Ischemia and Post-conditioning—To identify key regulator genes and to visualize the affected pathways in ischemic plus post-conditioned compared to ischemic plus sham post-conditioned retinae, iPathwayGuide [19] (Advaita, Plymouth, MI, USA) – a web-based impact analysis [20] tool was used. It utilizes the Kyoto Encyclopedia of Genes and Genomes (KEGG) [21] pathway database for molecular pathway representation, with results from edgeR pairwise comparisons (fold changes and Q values) as input. As opposed to functional analysis tools, iPathwayGuide takes into account the position of each gene on each pathway, and the type and directions of the interactions with the other genes. iPathwayGuide deems genes significantly altered if Q   0.05 and absolute value of $\log_2$(fold change)   2. Significantly affected pathways with adjusted P values, or FDR (false discovery rate)   0.05 were obtained from two of our comparison groups, i.e., PCI *vs* ShamN and ShamI *vs* ShamN, and were analyzed for uniqueness.

F) Downstream/Upstream Target Identification in Ischemia and Post-conditioning—To determine the overall changes between specific genes in our unique pathways, each pathway was analyzed with respect to the number, location and fold change difference of significantly up-regulated/down-regulated genes *vs* the other group.

RESULTS

1) Data Quality

Low count-filtered, TMM and cpm-normalized, $\log_2$-transformed table of counts was used to generate boxplots (Fig 1) [22] visualizing the relative abundance of gene expression between samples. Results confirmed that the distribution of expression of individual genes was similar across the samples. Principal Component Analysis (PCA) [23] of the first two principal components and clustering image map of distances between samples demonstrated the variance between sample groups and sample replicates (Fig 2) [22]. PCA plots of additional components are available in the Data Supplement (Supp. Fig 1, Supp. Fig 2). The results indicated a relative homogeneity between samples within their biological groups with minimal variation.

2) Differential Gene Expression in Ischemia with Post-C or sham Post-C

The overall results of the differential gene expression of PCI *vs* ShamN and ShamI *vs* ShamN are illustrated by their respective volcano plots (Supp. Fig 4, Supp. Fig 5) [24]. There were 1352 differentially expressed genes (DEGs), of which 332 were down-regulated and 1020 up-regulated in PCI *vs* ShamN, and 416 DEGs, with 46 down-regulated and 370 up-regulated in ShamI *vs* ShamN. The 4-way Venn diagram (Fig 3) summarizes the raw number of DEGs in each of the groups. The Supplemental Tables 8–11, and website link https://uofi.box.com/s/7cpuceq42fz0tk6jpgp8e9cvl9fiv2in contain the full set of data from which Fig 3 was derived. From Fig 3, 692 genes were uniquely up-regulated in PCI *vs* ShamN in contrast to 41 in ShamI *vs* ShamN. The vast majority of up-regulated genes in ShamI *vs* ShamN, were also up-regulated in PCI *vs* ShamN (328 genes). Similarly, 300

genes were significantly down-regulated in PCI *vs* ShamN and 15 in ShamI vs ShamN. The overall number of DEGs was much higher in PCI *vs* ShamN in contrast to ShamI *vs* ShamN. The top 20 DEGs arranged in ascending order of Q values, for PCI *vs* ShamN and ShamI *vs* ShamN are shown in Table 1 with their respective gene IDs and gene names.

3) Functional Analysis of Ischemia with Post-C or sham Post-C

The top 10 (ordered by P value) biological processes and molecular functions for PCI *vs* ShamN as well as ShamI *vs* ShamN are displayed in Figs 4 & Fig 5, respectively. For PCI vs. ShamN, the highest % of genes making up the biological processes were: response to drug (7.4%; of course no drugs were used in this study, but common pathways may be detected), inflammatory response (6.5%), response to lipopolysaccharides (5.2%), and immune response (4.5%), while for molecular functions they included: protein binding (15.3%), identical protein binding (9.2%), protein homo-dimerization activity (7.4%) and protein kinase binding (4.6%). For ShamI vs ShamN, the biological processes with the highest % of differentially expressed genes included: inflammatory response (9.6%), immune response (7.4%), innate immune response (6.6%) and cellular response to lipopolysaccharide (6.4%), while for molecular functions they were: protein binding (14.5%), protein homo-dimerization activity (8.6%), carbohydrate binding (3.4%) and integrin binding (2.9%). In addition, the top 10 (ordered by P value) biological processes and molecular functions uniquely affected in PCI *vs* ShamN in comparison to ShamI *vs* ShamN are displayed in Fig 6. Biological processes involving the highest % of groups included: positive regulation of transcription from RNA polymerase II promoter (7.9%), negative regulation of gene expression (2.6%), protein auto-phosphorylation (2.2%) and positive regulation of neuron projection development (2%), while for molecular functions, we obtained: ATP binding (10.33%), protein kinase binding (4.6%), protein C-terminus binding (2.2%) and calmodulin binding (2.2%).

4) Pathway/Impact Analysis in Ischemia with Post-C or sham Post-C

There were 71 significantly affected pathways in PCI *vs* ShamN and 43 in ShamI *vs* ShamN. Of these, 28 were unique to PCI *vs* ShamN. Table 2 summarizes the significantly affected pathways across our conditions. Of 28 uniquely affected pathways in PCI *vs* ShamN, 7 were chosen for further analysis due to their known or potential biological relevance to ischemic injury. These included: MAPK, apoptosis, Jak-STAT, PI3K-Akt, HIF-1, p53 and cell cycle.

5) Downstream/Upstream Potential Target Identification in Ischemia with Post-C or sham Post-C

The 7 unique pathway diagrams for PCI *vs* ShamN were juxtaposed to ShamI *vs* ShamN for comparison. They represent the overall positions and fold changes of the significantly affected genes in a chosen pathway for both groups. Genes were deemed significantly up-regulated if $\log_2$(fold change) $\geq$ 2 & Q $\leq$ 0.05, and significantly down-regulated if $\log_2$(fold change) $\leq$ −2 & Q $\leq$ 0.05. Diagrams present the up-regulated genes in red and down-regulated genes in blue.

To illustrate, the Jak-Stat KEGG pathway diagrams for PCI *vs* ShamN (Fig 7) and ShamI *vs* ShamN (Fig 8) are presented. Genes uniquely up-regulated for PCI *vs* ShamN were: Socs3,

Cdkn1a, Myc, Stat6, Jak2, Ifngr2, Il6r, Csf2ra, Il2rg, Il13ra2, Csf3r, Csf2rb, Il23a, Il11, Il6, and Csf2. (Table 3).

MAPK KEGG pathway diagrams for PCI *vs* ShamN (Supp. Fig 6) and ShamI *vs* ShamN (Supp. Fig 7) are presented. The MAPK KEGG pathway diagram yielded uniquely up-regulated genes in PCI *vs* ShamN: Dusp16, Dusp6, Dusp10, Dusp2, Gng12, Rps6ka1, Tgfb1, Rac2, Mapkapk3, Mknk1, Il1r2, Myc, Tnf, Nfkb1, Nfkb2, Fas, Map3k8, Map4k4, Gadd45b, and Fos. Fgf14 and Cacng2 were uniquely down-regulated in PCI *vs* ShamN. (Supp. Table 2).

Apoptosis KEGG pathway diagrams for PCI *vs* ShamN and ShamI *vs* ShamN (Supp. Fig 8 & Supp. Fig 9) respectively, revealed uniquely up-regulated genes in PCI *vs* ShamN: Traf1, Tnfrsf1a, Tnf, Parp3, Nfkbia, Nfkb1, Hrk, Gadd45b, Fos, Fas, Csf2rb, Cflar, Birc5, Birc3, Bak1 and Actb. (Supp. Table 3).

PI3K-Akt KEGG pathway diagrams (Supp. Fig 10 & Supp. Fig 11) showed uniquely up-regulated genes in PCI *vs* ShamN: Nfkb1, Creb5, Cdkn1a, Myc, Pik3cd, Gng12, Itgb7, Itga4, Itga5, Lamc1, Thbs3, Jak2, Il6r, Il2rg, Csf3r, Il6, Csf3, Pik3ap1, Syk, Met, Epha2, Csf1 and Angpt4. Fgf14 was down-regulated in PCI *vs* ShamN. Chrm2 was the only gene uniquely affected in ShamI *vs* ShamN (down-regulated, Supp. Table 4).

HIF-1 KEGG pathway diagrams (Supp. Fig 12& Supp. Fig 13) showed a set of uniquely up-regulated genes in PCI *vs* ShamN: Nos2, Nfkb1, Mknk1, Il6r, Il6, Hk3, Egln3, Cdkn1a, and Angpt4 (Supp. Table 5).

p53 KEGG pathway diagrams (Supp.Fig 14 & Supp. Fig 15), represent the overall positions and fold changes of the significantly up-regulated genes in the HIF-1 pathway for PCI *vs* ShamN and ShamI *vs* ShamN respectively. They revealed a set of uniquely up-regulated genes in PCI *vs* ShamN: Igfbp3, Cd82, Fas, Cdkn1a, Cdk1, Gadd45b, and Ccnb1. (Supp. Table 6).

Cell cycle KEGG pathway diagrams (Supp. Fig 16 & Supp. Fig 17) demonstrated genes that were uniquely up-regulated for PCI *vs* ShamN: Tgfb1, Myc, Mcm5, Cdkn1a, Cdk1, Gadd45b, Ccnb1, Bub1b, Pttg1, Mcm6, and Mcm3. (Supp. Table 7).

DISCUSSION

RNA-Seq profiling of the transcriptome of the whole retina yielded 17,300 genes. RNA-Seq is the optimal method for large-scale transcription analysis as it quantitates gene expression, enables novel gene discovery, and detects low abundance genes in a tissue such as the retina [25]. We observed significant differences in both the identities of, degree of changes in, and the pathways of differentially expressed genes in postconditioning following ischemia compared to sham post-conditioning following ischemia. Differentially expressed genes were then subsequently classified according to their biological processes and molecular functions. The results yield important clues regarding the molecular machinery of this remarkable endogenous protective mechanism in the retina. While we cannot state at this

time with certainty which of these pathways will be therapeutically accessible, there are some promising candidates based upon existing studies.

Pathway analysis using iPathwayGuide[TM] [19] yielded 28 uniquely affected pathways in PCI *vs* ShamN. We chose seven specific pathways for further study of mechanisms of Post-C. These included MAPK, apoptosis, Jak-STAT, PI3K-Akt, HIF-1, p53 and cell cycle. Some of the genes overlap across the pathways, thus to simplify presentation, p53 and cell cycle pathways are combined in this Discussion.

These pathways were chosen based on previous studies suggesting biological relevance to ischemia, neuroprotection, or pre- or post-conditioning. Apoptosis is a common mechanism mediating cell death. We previously described that apoptosis peaks in the retina approximately 24–48 h after ischemia [26, 27]. Thus, the retinas were collected at 24 h after Post-C (48 h after ischemia), consistent with the previously described time course of apoptosis. We hypothesized that Post-C significantly attenuated ischemia-induced apoptosis-related gene expression. All of the genes present in Supp. Table 3 had significantly increased expression in PCI vs ShamN compared to ShamI vs Sham N. Some of these genes (e.g., Cflar, Gadd45b, Nfkbia, Birc3 and 5, and Nfkb1) are known anti-apoptosis, pro-survival genes, while others (e.g., Fos, Parp3, Fas, and Tnfrsf1a [28, 29]) are pro-apoptotic. Therefore, it is likely that survival or death from apoptosis is dependent upon a balance of these pro- and anti-apoptosis genes, and may also depend upon the timing of their expression, not specifically addressed in this study, where we only measured gene expression at one time point.

In the p53 pathway/cell cycle, eight genes were significantly increased in PCI vs ShamN, but not in ShamI vs ShamN: Ccnb1, Gadd45b and Gadd45g (overlapping with apoptosis gene expression), Cdk1, Cdkn1a, Fas (also overlapping with apoptosis gene expression), Igfbp3 and Cd82. The cell cycle pathway had: Myc, Ccnb1, Tgfb1, Cdkn1a, Bub1b, Pttg1, Cdk1, Gadd45b and g, and Mcm3, 5, and 6. Relatively little is known about cell cycle regulators and ischemic injury in the retina, rendering these results novel. Kuroiwa et al[30] showed increases in Ccnd1 at 24 h after retinal ischemia in rats, but the functional significance of the changes has not been described. Under normal conditions, neurons are post-mitotic and do not re-enter the cell cycle. However, following cerebral ischemia in rats, neurons resumed DNA synthesis as indicated by bromo-deoxyuridine (BrdU) incorporation and expression of G1/S-phase cell cycle transition markers, and were TUNEL positive, suggesting that they underwent apoptosis. BrdU+/TUNEL neurons had decreased G1-phase cyclin-dependent kinase (CDK) inhibitors Cdkn2a and Cdkn1b, induction of late G1/S-phase Cdk2 activity, and retinoblastoma protein phosphorylation [31]. It is difficult to explain why myc and Cdkn1a, with opposite effects on cell cycling, changed in the same direction, and further studies will be necessary to clarify the implications of these findings.

Notable in our results is that ischemic and post-conditioned retinas had increased Ccnb1, Cdk1, Cdkn1a, and Gadd45b. Ccnb1 regulates G2 to M transition, and Cdk1 favors cell cycle arrest in G2 phase, Gadd45 is involved in DNA repair and damage prevention, and Cdkn1a inhibits entrance into the cell cycle by blocking Ccnd1 and Cdk4/6 [32]. This

suggests but does not prove, the possibility that Post-C prevents entrance or completion of the cell cycle in ischemia, and favors DNA repair, to prevent apoptosis and cell death.

With respect to the other cell cycle/p53 genes, Pttg1 de-regulation has recently been observed in several mouse models of retinal degeneration, [33, 34] suggesting a possible cell survival role in retina. Bub1b is a component of the mitotic spindle checkpoint, which prevents sister chromatid separation during cell division. Abnormal Bub1b signaling has been implicated in premature aging, although to date, no studies have addressed its role in retina [35, 36]. MCM proteins control DNA unwinding. [37] In retina, Mcm5 depletion resulted in apoptosis, likewise suggesting an essential survival function [38]. Because of the prominence of apoptosis in the damage from retinal ischemia, the p53 pathway may be a viable drug target. [39]

In the HIF-1 pathway, increases were found in Angpt4, Cdkn1a [40], Egln3, Hk3, Ifngr2, Il6, Il6r, Mknk1, Nfkb1, and Nos2. Cdkn1a has been associated with neuroprotection in cortical neurons subjected to oxidative stress as well as in a cerebral ischemia model in vivo [40]. Angpt4 has been identified as an angiogenic factor in diabetic retinopathy [41] and increases permeability while enhancing survival of endothelial cells [42]. With respect to Egln3 [43], HIF is regulated by prolyl hydroxylases, which induces hydroxylation on proline-402 and -564 on the HIFα subunit [44]. Inhibiting Egln3 prevented oxygen induced retinopathy [45]. However, blockade of Egln3 enhanced HIF1 and decreased myocardial infarct size [46], thus the significance of increased Egln3 in our study remains unclear.

JAK-STAT cytokines and their receptors, Jak2, Stat6, Myc, Cdkn1a, and Socs3 demonstrated increases. There is evidence implicating the JAK-STAT pathway in both neuroprotection from cerebral ischemia, and in myocardial preservation after ischemia. Specifically, the JAK-STAT pathway was involved in Post-C preventing damage from global cerebral ischemia and myocardial ischemia [47–50], suggesting a possible role in retinal ischemic Post-C as well. But there are novel genes in the pathway identified in this study which have not been previously studied in ischemic injury or neuroprotection, including Il23a and Csf2, which may be drug targets to examine in future studies.

For MAPK, previously, members of the pathway have been implicated in ischemic injury, pre- and post-ischemic conditioning [51]. But several novel genes were identified in this study. Fgf14 is a novel protein controlling channel gating, axonal targeting and phosphorylation in neurons, affecting synaptic transmission, plasticity and neurogenesis. To date, its role in retina or in ischemia has not been evaluated, although it may be involved in neurodegeneration [52, 53]. Cacng2 is an AMPA-receptor regulating protein [54]. Map4k4 and Map3k8 are inflammatory kinases; Map4k4 also inhibits Jnk. Their role in ischemia has not been previously studied [55–57].

Given our previously demonstrated essential role of Akt in retinal Post-C [7], it was not surprising that the PI3K-Akt pathway had a large number of differentially regulated genes in ischemia and Post-C. Many of these, such as the growth factors (e.g., Fgf14), the cytokines (e.g., Il6r, Il6), integrins (e.g., Itga4), receptor tyrosine kinase (e.g., Epha2), are involved in binding to cellular receptors and activation of the PI3K and Akt signaling pathways [58]. We

also noted increases in downstream signals in PCI vs ShamN, including those involved in cell cycle regulation (e.g., Myc and Cdkn1a) [32], and cell survival mechanisms (e.g., Nfkb1, and Creb5) [59]. Excepting Nfkb1, these downstream factors have not been previously studied for a role in ischemic neuroprotection in the retina.

Complicating interpretation of our results is that we are unable to determine the role of specific retinal cells, since we studied the transcriptome in the whole retina. Importantly, neurons and Muller cells may behave differently after injury. Müller glial cells are the major support cell for neurons in the vertebrate retina. Following neuronal damage, Müller cells undergo reactive gliosis, characterized by proliferation and changes in gene expression. Downregulation of the tumor suppressor protein p27Kip1 and re-entry into the cell cycle occur within the first 24 hours after retinal injury. Müller glial cells upregulate genes for gliosis and then downregulate cyclin D3 [60]. Therefore, we could miss important effects specific to Muller cells. This has important implications for cell survival and regeneration of retina, because in mice, if neuronal death is coupled with the intraocular injection of growth factors, Müller glia dedifferentiate, enter the cell cycle, and support modest neuronal regeneration [61]. However, to date true neuronal regeneration from Muller cells has not been shown in mammalian retina. [62]

Comparing these results to descriptions of gene expression in human retina in diabetic retinopathy, ARM, and central retinal artery occlusion is complicated by the use of different measurement methods (e.g. microarray vs our use of RNA-seq), different sampling methods, and smaller sample sizes. However, it is of interest that in a study of fibrovascular membranes from patients with proliferative diabetic retinopathy, several of these pathways overlapped with ours including apoptosis, cell cycle, and immune response.[63]

The advantages and challenges of RNA-Seq have been reviewed elsewhere [9]. RNA-Seq also has drawbacks which may limit the implications of our results. Library construction remains a challenge [9], because it involves a number of discrete steps, each of which brings a set of unique complications. Library preparation may introduce noise, and skew read distribution. Long reads and shallow read depth are important trade-offs that could have affected our results [64]. Large or complex transcriptomes genome alignment poses significant computational and technical challenges. In complex transcriptomes, alternative splicing and splice junctions make reads difficult to map while for large transcriptomes a significant portion of reads map to the multiple locations of the genome [9]. For our experiment specifically, the main drawback is that RNA-Seq is a snapshot of the ever-shifting nature of the cell's transcriptome and it might not be reflective of events over time. For this reason we chose a 24h post-ischemia period as our point of reference, which has been previously shown to be the peak time of apoptosis as well as the optimal time for treatment [2].

The results of this experiment have elucidated pathways as well as specific genes that may be involved in retinal ischemic post-conditioning. Studying the impact of increasing expression of these factors may yield insight into new methods for treating or preventing damage from retinal ischemic disorders.

Supplementary Material

Refer to Web version on PubMed Central for supplementary material.

Acknowledgments

References

1. Zheng L, Gong B, Hatala DA, Kern TS. Retinal ischemia and reperfusion causes capillary degeneration: similarities to diabetes. Invest Ophthalmol Vis Sci. 2007; 48:361–367. [PubMed: 17197555]

2. Dreixler JC, Poston JN, Shaikh AR, Alexander M, Tupper KY, Marcet MM, Bernaudin M, Roth S. Delayed post-ischemic conditioning significantly improves the outcome after retinal ischemia. ExpEye Res. 2011; 92:521–527. DOI: 10.1016/j.exer.2011.03.015

3. Fernandez DC, Bordone MP, Chianelli MS, Rosenstein RE. Retinal neuroprotection against ischemia-reperfusion damage induced by postconditioning. Invest Ophthalmol Vis Sci. 2009; 50:3922–3930. [PubMed: 19339733]

4. Osborne NN, Ugarte M, Chao M, Chidlow G, Bae JH, Wood JP, Nash MS. Neuroprotection in relation to retinal ischemia and relevance to glaucoma. Surv Ophthalmol. 1999; 43(Suppl 1):S102–128. [PubMed: 10416754]

5. Limalanathan S, Andersen GO, Hoffmann P, Klow N-E, Abdelnoor M, Eritsland J. Rationale and design of the POSTEMI (postconditioning in ST-elevation myocardial infarction) study. Cardiology. 2010; 116:103–109. [PubMed: 20588018]

6. Zhao H. Ischemic postconditioning as a novel avenue to protect against brain injury after stroke. J CerebBlood Flow Metabol. 2009; 29:873–885.

7. Dreixler JC, Sampat A, Shaikh AR, Alexander M, Marcet MM, Roth S. Protein kinase B (Akt) and mitogen-activated protein kinase p38alpha in retinal ischemic post-conditioning. J Mol Neurosci. 2011; 45:309–320. DOI: 10.1007/s12031-011-9523-5 [PubMed: 21573888]

8. Yasuda M, Tanaka Y, Omodaka K, Nishiguchi KM, Nakamura O, Tsuda S, Nakazawa T. Transcriptome profiling of the rat retina after optic nerve transection. Sci Rep. 2016; 6:28736.doi: 10.1038/srep28736 [PubMed: 27353354]

9. Wang Z, Gerstein M, Snyder M. RNA-Seq: a revolutionary tool for transcriptomics. Nat Rev Genet. 2009; 10:57–63. DOI: 10.1038/nrg2484 [PubMed: 19015660]

10. Brown J, Pirrung M, McCue LA. FQC Dashboard: Integrates FastQC results into a web based interactive and extensible FastQ quality control tool. Bioinformatics. 2017; Epub ahead of print. doi: 10.1093/bioinformatics/btx373

11. Li H, Durbin R. Fast and accurate long-read alignment with Burrows-Wheeler transform. Bioinformatics. 2010; 26:589–595. DOI: 10.1093/bioinformatics/btp698 [PubMed: 20080505]

12. Liao Y, Smyth GK, Shi W. featureCounts: an efficient general purpose program for assigning sequence reads to genomic features. Bioinformatics. 2014; 30:923–930. DOI: 10.1093/bioinformatics/btt656 [PubMed: 24227677]

13. Robinson MD, McCarthy DJ, Smyth GK. edgeR: a Bioconductor package for differential expression analysis of digital gene expression data. Bioinformatics. 2010; 26:139–140. DOI: 10.1093/bioinformatics/btp616 [PubMed: 19910308]

14. Anders S, McCarthy DJ, Chen Y, Okoniewski M, Smyth GK, Huber W, Robinson MD. Count-based differential expression analysis of RNA sequencing data using R and Bioconductor. Nat Protoc. 2013; 8:1765–1786. DOI: 10.1038/nprot.2013.099 [PubMed: 23975260]

15. Benjamini Y, Hochberg Y. Controlling the False Discovery Rate: A Practical and Powerful Approach to Multiple Testing. JRoyal StatSoc Series B (Methodological). 1995; 57:289–300.

16. Pathan M, Keerthikumar S, Ang CS, Gangoda L, Quek CY, Williamson NA, Mouradov D, Sieber OM, Simpson RJ, Salim A, Bacic A, Hill AF, Stroud DA, Ryan MT, Agbinya JI, Mariadason JM, Burgess AW, Mathivanan S. FunRich: An open access standalone functional enrichment and interaction network analysis tool. Proteomics. 2015; 15:2597–2601. DOI: 10.1002/pmic. 201400515 [PubMed: 25921073]

17. Ashburner M, Ball CA, Blake JA, Botstein D, Butler H, Cherry JM, Davis AP, Dolinski K, Dwight SS, Eppig JT, Harris MA, Hill DP, Issel-Tarver L, Kasarskis A, Lewis S, Matese JC, Richardson JE, Ringwald M, Rubin GM, Sherlock G. Gene ontology: tool for the unification of biology. The Gene Ontology Consortium. Nat Genet. 2000; 25:25–29. DOI: 10.1038/75556 [PubMed: 10802651]

18. Collaborators. Gene Ontology Consortium: going forward. Nucleic Acids Res. 2015; 43:D1049–1056. DOI: 10.1093/nar/gku1179 [PubMed: 25428369]

19. Ahsan S, Draghici S. Identifying Significantly Impacted Pathways and Putative Mechanisms with iPathwayGuide. Curr Protoc Bioinformatics. 2017; 57:7.15.1–7.15.30. DOI: 10.1002/cpbi.24 [PubMed: 28654712]

20. Draghici S, Khatri P, Tarca AL, Amin K, Done A, Voichita C, Georgescu C, Romero R. A systems biology approach for pathway level analysis. Genome Res. 2007; 17:1537–1545. DOI: 10.1101/gr. 6202607 [PubMed: 17785539]

21. Kanehisa M, Goto S. KEGG: kyoto encyclopedia of genes and genomes. Nucleic Acids Res. 2000; 28:27–30. [PubMed: 10592173]

22. Huang HC, Niu Y, Qin LX. Differential Expression Analysis for RNA-Seq: An Overview of Statistical Methods and Computational Software. Cancer Inform. 2015; 14(Suppl 1):57–67. DOI: 10.4137/CIN.S21631

23. Hussein SMI, Puri MC, Tonge PD, Benevento M, Corso AJ, Clancy JL, Mosbergen R, Li M, Lee D-S, Cloonan N, Wood DLA, Munoz J, Middleton R, Korn O, Patel HR, White CA, Shin J-Y, Gauthier ME, Cao K-AL, Kim J-I, Mar JC, Shakiba N, Ritchie W, Rasko JEJ, Grimmond SM, Zandstra PW, Wells CA, Preiss T, Seo J-S, Heck AJR, Rogers IM, Nagy A. Genome-wide characterization of the routes to pluripotency. Nature. 2014; 516:198–206. DOI: 10.1038/nature14046 [PubMed: 25503233]

24. Li W. Volcano plots in analyzing differential expressions with mRNA microarrays. J Bioinform Comput Biol. 2012; 10:1231003.doi: 10.1142/S0219720012310038 [PubMed: 23075208]

25. Wang C, Gong B, Bushel PR, Thierry-Mieg J, Thierry-Mieg D, Xu J, Fang H, Hong H, Shen J, Su Z, Meehan J, Li X, Yang L, Li H, Labaj PP, Kreil DP, Megherbi D, Gaj S, Caiment F, van Delft J, Kleinjans J, Scherer A, Devanarayan V, Wang J, Yang Y, Qian H-R, Lancashire LJ, Bessarabova M, Nikolsky Y, Furlanello C, Chierici M, Albanese D, Jurman G, Riccadonna S, Filosi M, Visintainer R, Zhang KK, Li J, Hsieh J-H, Svoboda DL, Fuscoe JC, Deng Y, Shi L, Paules RS, Auerbach SS, Tong W. The concordance between RNA-seq and microarray data depends on chemical treatment and transcript abundance. Nat Biotech. 2014; 32:926–932. DOI: 10.1038/nbt. 3001

26. Zhang C, Rosenbaum DM, Shaikh AR, QL, Rosenbaum PS, Pelham DJ, Roth S. Ischemic preconditioning attenuates apoptosis following retinal ischemia in rats. Invest Ophthalmol Vis Sci. 2002; 43:3059–3066. [PubMed: 12202530]

27. Singh M, Savitz SI, Hoque R, Rosenbaum PS, Roth S, Rosenbaum DM. Cell-specific caspase expression by different neuronal phenotypes in transient retinal ischemia. J Neurochem. 2001; 77:466–475. [PubMed: 11299309]

28. Berger S, Savitz SI, Nijhawan S, Singh M, David J, Rosenbaum PS, Rosenbaum DM. Deleterious role of TNF-alpha in retinal ischemia-reperfusion injury. Invest Ophthalmol Vis Sci. 2008; 49:3605–3610. DOI: 10.1167/iovs.07-0817 [PubMed: 18660426]

29. Wan T, Xu Z, Zhou HJ, Zhang H, Luo Y, Li Y, Min W. Functional analyses of TNFR2 in physiological and pathological retina angiogenesis. Invest Ophthalmol Vis Sci. 2013; 54:211–221. DOI: 10.1167/iovs.12-10364 [PubMed: 23188724]

30. Kuroiwa S, Katai N, Shibuki H, Kurokawa T, Umihira J, Nikaido T, Kametani K, Yoshimura N. Expression of cell cycle-related genes in dying cells in retinal ischemic injury. Invest Ophthalmol Vis Sci. 1998; 39:610–617. [PubMed: 9501873]

31. Kuan CY, Schloemer AJ, Lu A, Burns KA, Weng WL, Williams MT, Strauss KI, Vorhees CV, Flavell RA, Davis RJ, Sharp FR, Rakic P. Hypoxia-ischemia induces DNA synthesis without cell proliferation in dying neurons in adult rodent brain. J Neurosci. 2004; 24:10763–10772. DOI: 10.1523/jneurosci.3883-04.2004 [PubMed: 15564594]

32. Frade JM, Ovejero-Benito MC. Neuronal cell cycle: the neuron itself and its circumstances. Cell Cycle. 2015; 14:712–720. DOI: 10.1080/15384101.2015.1004937 [PubMed: 25590687]

33. Keeley PW, Zhou C, Lu L, Williams RW, Melmed S, Reese BE. Pituitary tumor-transforming gene 1 regulates the patterning of retinal mosaics. Proc Natl AcadSciUSA. 2014; 111:9295–9300. DOI: 10.1073/pnas.1323543111

34. Yetemian RM, Craft CM. Characterization of the pituitary tumor transforming gene 1 knockout mouse retina. Neurochem Res. 2011; 36:636–644. DOI: 10.1007/s11064-010-0334-9 [PubMed: 21203837]

35. Matsuda D, Matsumoto T, Honma K, Ikawa-Yoshida A, Onimaru M, Furuyama T, Nakatsu Y, Tsuzuki T, Maehara Y. BUBR1 Insufficiency in Mice Increases their Sensitivity to Oxidative Stress. In Vivo. 2016; 30:769–776. [PubMed: 27815460]

36. Yang Z, Jun H, Choi CI, Yoo KH, Cho CH, Hussaini SMQ, Simmons AJ, Kim S, van Deursen JM, Baker DJ, Jang MH. Age-related decline in BubR1 impairs adult hippocampal neurogenesis. Aging Cell. 2017; 16:598–601. DOI: 10.1111/acel.12594 [PubMed: 28383136]

37. Deegan TD, Diffley JF. MCM: one ring to rule them all. Curr Opin Struct Biol. 2016; 37:145–151. DOI: 10.1016/j.sbi.2016.01.014 [PubMed: 26866665]

38. Ryu S, Holzschuh J, Erhardt S, Ettl AK, Driever W. Depletion of minichromosome maintenance protein 5 in the zebrafish retina causes cell-cycle defect and apoptosis. ProceNatl AcadSciUSA. 2005; 102:18467–18472. DOI: 10.1073/pnas.0506187102

39. Nivison-Smith L, Khoo P, Acosta ML, Kalloniatis M. Vinpocetine protects inner retinal neurons with functional NMDA glutamate receptors against retinal ischemia. Exp Eye Res. 2017; 167:1–13. DOI: 10.1016/j.exer.2017.10.008 [PubMed: 29106899]

40. Langley B, D'Annibale MA, Suh K, Ayoub I, Tolhurst A, Bastan B, Yang L, Ko B, Fisher M, Cho S, Beal MF, Ratan RR. Pulse inhibition of histone deacetylases induces complete resistance to oxidative death in cortical neurons without toxicity and reveals a role for cytoplasmic p21(waf1/cip1) in cell cycle-independent neuroprotection. J Neurosci. 2008; 28:163–176. DOI: 10.1523/jneurosci.3200-07.2008 [PubMed: 18171934]

41. Babapoor-Farrokhran S, Jee K, Puchner B, Hassan SJ, Xin X, Rodrigues M, Kashiwabuchi F, Ma T, Hu K, Deshpande M, Daoud Y, Solomon S, Wenick A, Lutty GA, Semenza GL, Montaner S, Sodhi A. Angiopoietin-like 4 is a potent angiogenic factor and a novel therapeutic target for patients with proliferative diabetic retinopathy. Proc Natl Acad Sci USA. 2015; 112:E3030–3039. DOI: 10.1073/pnas.1423765112 [PubMed: 26039997]

42. Kesler CT, Pereira ER, Cui CH, Nelson GM, Masuck DJ, Baish JW, Padera TP. Angiopoietin-4 increases permeability of blood vessels and promotes lymphatic dilation. Faseb J. 2015; 29:3668–3677. DOI: 10.1096/fj.14-268920 [PubMed: 25977256]

43. Jaakkola PM, Rantanen K. The regulation, localization, and functions of oxygen-sensing prolyl hydroxylase PHD3. Biol Chem. 2013; 394:449–457. DOI: 10.1515/hsz-2012-0330 [PubMed: 23380539]

44. Yu F, White SB, Zhao Q, Lee FS. HIF-1alpha binding to VHL is regulated by stimulus-sensitive proline hydroxylation. Proc Natl Acad Sci USA. 2001; 98:9630–9635. DOI: 10.1073/pnas.181341498 [PubMed: 11504942]

45. Trichonas G, Lee TJ, Hoppe G, Au J, Sears JE. Prolyl hydroxylase inhibition during hyperoxia prevents oxygen-induced retinopathy in the rat 50/10 model. Invest Ophthalmol Vis Sci. 2013; 54:4919–4926. DOI: 10.1167/iovs.13-12171 [PubMed: 23761085]

46. Vogler M, Zieseniss A, Hesse AR, Levent E, Tiburcy M, Heinze E, Burzlaff N, Schley G, Eckardt KU, Willam C, Katschinski DM. Pre- and post-conditional inhibition of prolyl-4-hydroxylase domain enzymes protects the heart from an ischemic insult. Pflugers Arch. 2015; 467:2141–2149. DOI: 10.1007/s00424-014-1667-z [PubMed: 25578858]

47. Goodman MD, Koch SE, Fuller-Bicer GA, Butler KL. Regulating RISK: a role for JAK-STAT signaling in postconditioning? Am J Physiol. 2008; 295:H1649–1656. DOI: 10.1152/ajpheart. 00692.2008

48. Hausenloy DJ, Yellon DM. Survival kinases in ischemic preconditioning and postconditioning. Cardiovasc Res. 2006; 70:240–253. DOI: 10.1016/j.cardiores.2006.01.017 [PubMed: 16545352]

49. Kim HC, Kim E, Bae JI, Lee KH, Jeon YT, Hwang JW, Lim YJ, Min SW, Park HP. Sevoflurane Postconditioning Reduces Apoptosis by Activating the JAK-STAT Pathway After Transient Global Cerebral Ischemia in Rats. J Neurosurg Anesthesiol. 2017; 29:37–45. DOI: 10.1097/ana. 0000000000000331 [PubMed: 27337676]

50. Wang Y, Wang D, Zhang L, Ye F, Li M, Wen K. Role of JAK-STAT pathway in reducing cardiomyocytes hypoxia/reoxygenation injury induced by S1P postconditioning. Eur J Pharmacol. 2016; 784:129–136. DOI: 10.1016/j.ejphar.2016.05.024 [PubMed: 27215146]

51. Cox-Limpens KE, Gavilanes AW, Zimmermann LJ, Vles JS. Endogenous brain protection: what the cerebral transcriptome teaches us. Brain Res. 2014; 1564:85–100. DOI: 10.1016/j.brainres. 2014.04.001 [PubMed: 24713346]

52. Di Re J, Wadsworth PA, Laezza F. Intracellular Fibroblast Growth Factor 14: Emerging Risk Factor for Brain Disorders. Front Cell Neurosci. 2017; 11:103.doi: 10.3389/fncel.2017.00103 [PubMed: 28469558]

53. Pablo JL, Pitt GS. FGF14 is a regulator of KCNQ2/3 channels. Proc Natl Acad Sci USA. 2017; 114:154–159. DOI: 10.1073/pnas.1610158114 [PubMed: 27994149]

54. Ziff EB. TARPs and the AMPA receptor trafficking paradox. Neuron. 2007; 53:627–633. DOI: 10.1016/j.neuron.2007.02.006 [PubMed: 17329203]

55. Machida N, Umikawa M, Takei K, Sakima N, Myagmar BE, Taira K, Uezato H, Ogawa Y, Kariya K. Mitogen-activated protein kinase kinase kinase kinase 4 as a putative effector of Rap2 to activate the c-Jun N-terminal kinase. J Biol Chem. 2004; 279:15711–15714. DOI: 10.1074/jbc.C300542200 [PubMed: 14966141]

56. Roth Flach RJ, Skoura A, Matevossian A, Danai LV, Zheng W, Cortes C, Bhattacharya SK, Aouadi M, Hagan N, Yawe JC, Vangala P, Menendez LG, Cooper MP, Fitzgibbons TP, Buckbinder L, Czech MP. Endothelial protein kinase MAP4K4 promotes vascular inflammation and atherosclerosis. Nat Commun. 2015; 6:8995.doi: 10.1038/ncomms9995 [PubMed: 26688060]

57. Rowley SM, Kuriakose T, Dockery LM, Tran-Ngyuen T, Gingerich AD, Wei L, Watford WT. Tumor progression locus 2 (Tpl2) kinase promotes chemokine receptor expression and macrophage migration during acute inflammation. J Biol Chem. 2014; 289:15788–15797. DOI: 10.1074/jbc.M114.559344 [PubMed: 24713702]

58. Ghigo A, Laffargue M, Li M, Hirsch E. PI3K and Calcium Signaling in Cardiovascular Disease. Circ Res. 2017; 121:282–292. DOI: 10.1161/circresaha.117.310183 [PubMed: 28729453]

59. Carloni S, Girelli S, Scopa C, Buonocore G, Longini M, Balduini W. Activation of autophagy and Akt/CREB signaling play an equivalent role in the neuroprotective effect of rapamycin in neonatal hypoxia-ischemia. Autophagy. 2015; 6:366–377.

60. Dyer MA, Cepko CL. Control of Muller glial cell proliferation and activation following retinal injury. Nat Neurosci. 2000; 3:873–880. DOI: 10.1038/78774 [PubMed: 10966617]

61. Vetter ML, Hitchcock PF. Report on the National Eye Institute Audacious Goals Initiative: Replacement of Retinal Ganglion Cells from Endogenous Cell Sources. Transl Vis Sci Technol. 2017; 6:5.doi: 10.1167/tvst.6.2.5

62. Wilken MS, Reh TA. Retinal regeneration in birds and mice. Curr Opin Gen Devel. 2016; 40:57–64. DOI: 10.1016/j.gde.2016.05.028

63. Ishikawa K, Yoshida S, Kobayashi Y, Zhou Y, Nakama T, Nakao S, Sassa Y, Oshima Y, Niiro H, Akashi K, Kono T, Ishibashi T. Microarray Analysis of Gene Expression in Fibrovascular Membranes Excised From Patients With Proliferative Diabetic Retinopathy. Invest Ophthalmol Vis Sci. 2015; 56:932–946. DOI: 10.1167/iovs.14-15589 [PubMed: 25604687]
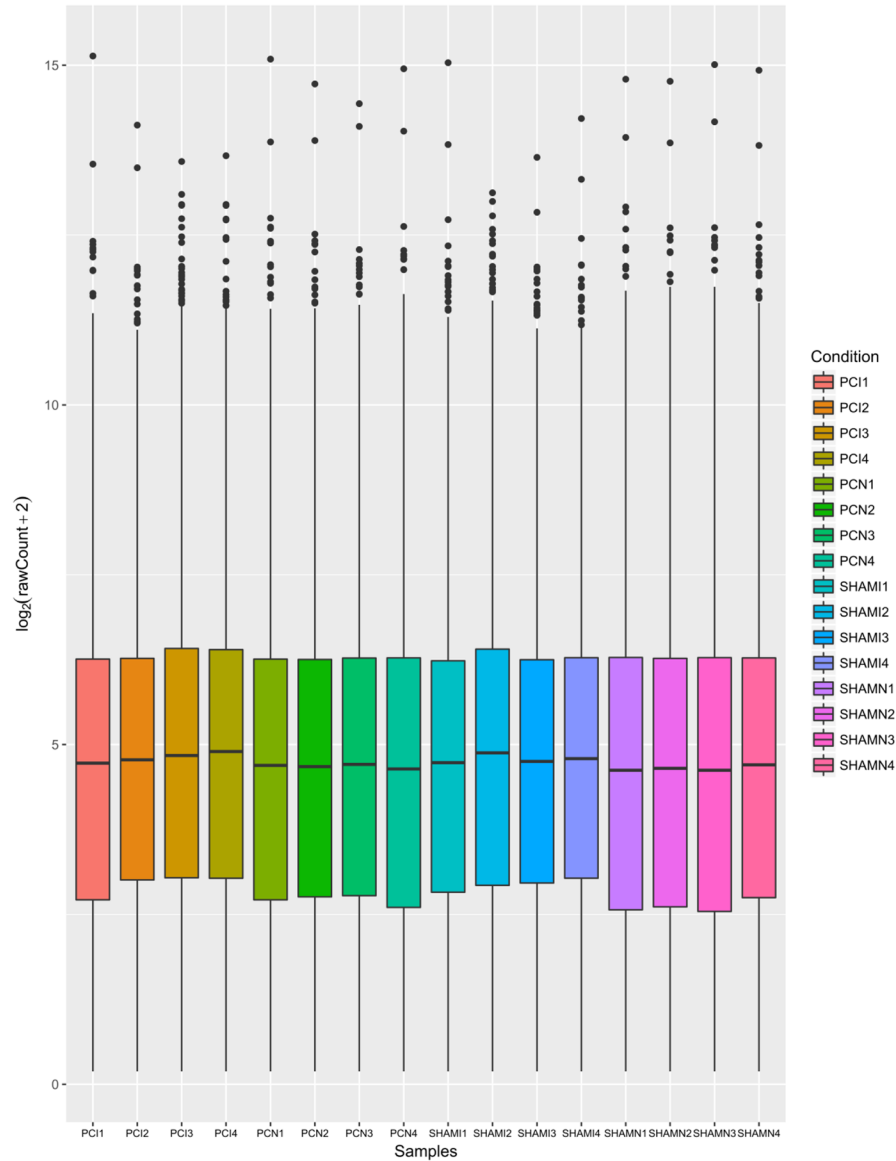
64. Kratz A, Carninci P. The devil in the details of RNA-seq. Nat Biotech. 2014; 32:882–884. DOI: 10.1038/nbt.3015

Fig. 1.
Gene expression in each sample, contrasting their respective distributions; generated using R v. 3.2.2 and ggplot2_2.2.1. Individual samples (x-axis) and their log2-transformed expression count (y-axis) are shown. Prior count of 2 was added in order to avoid log evaluation errors. Results confirm that the distribution of expression of individual genes is quite similar across the samples after normalization was performed, as well as that treatment did not have a profound effect at the genome-wide expression level.
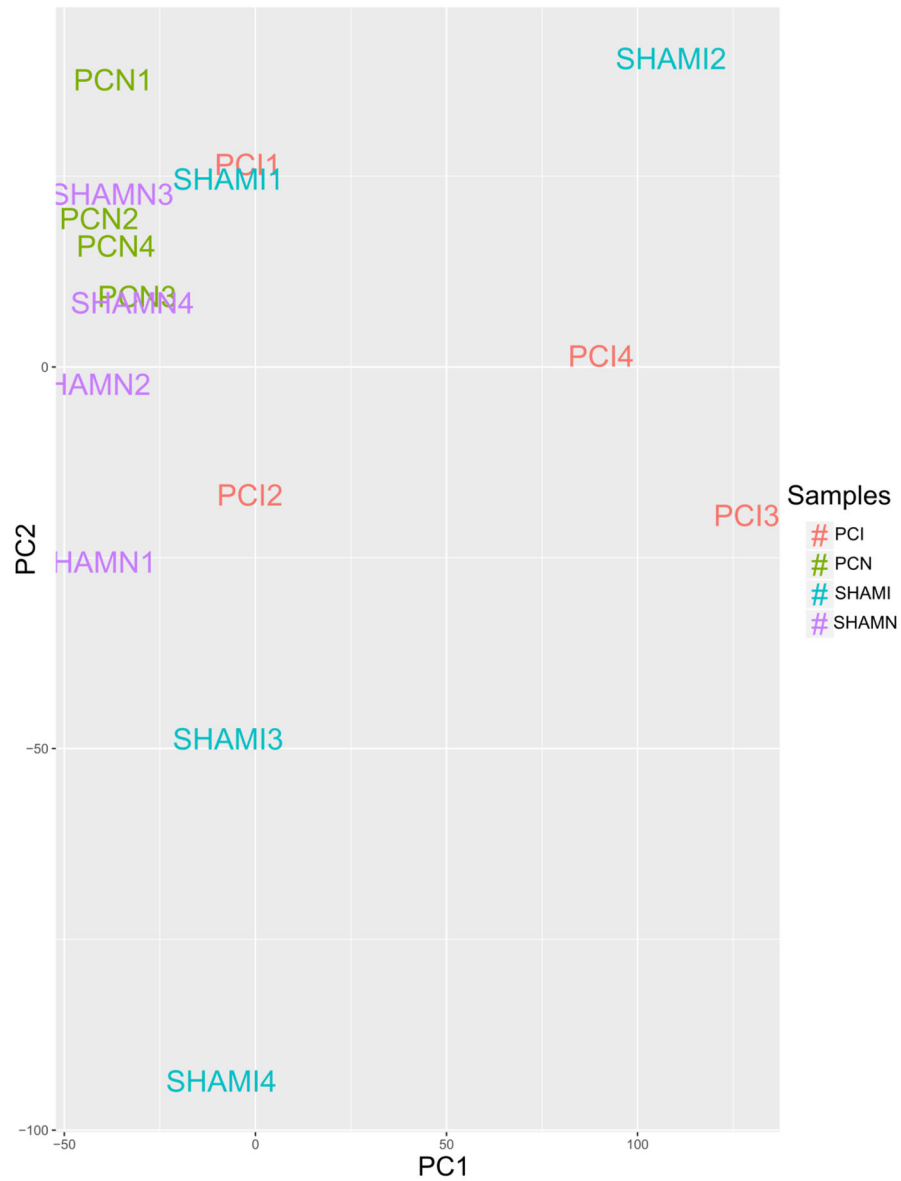
Fig. 2.

Principal Component Analysis (PCA) plot of the filtered, normalized and log$_2$-transformed count matrix, assessing the overall effect of experimental covariates and batch effects - generated with R v. 3.2.2, ggplot2_2.2.1 andggfortify_0.4.1. The first two components (x- and y-axis) were used and next order components are available in the Data Supplement. We noticed a higher variation in PCI3 and PCI4 and ShamI2, most likely due to natural variation in biological samples.
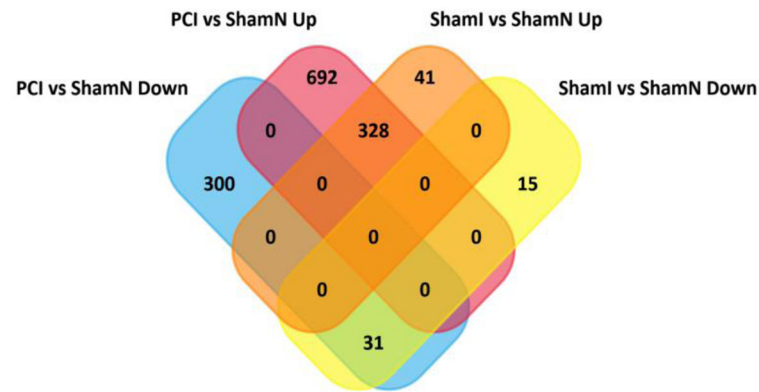
Fig. 3.
Four-way quantitative summary of the differential expression analysis results generated with FunRich 3.0. Overall, of 1352 DEGs present in PCI *vs* ShamN and 416 DEGs present in ShamI vs ShamN, 328 were up-regulated and 31 were down-regulated in both groups, while 692 genes were uniquely up-regulated in PCI *vs* ShamN in contrast to 41 in ShamI *vs* ShamN. The vast majority of up-regulated genes in ShamI *vs* ShamN, were also up-regulated in PCI *vs* ShamN (328 genes). Similarly, 300 genes were found to be significantly down-regulated in PCI *vs* ShamN to 15 in ShamI vs ShamN. See Supplemental Tables 8–11 for the complete data set used to construct Fig 3. https://uofi.box.com/s/7cpuceq42fz0tk6jpgp8e9cvl9fiv2in
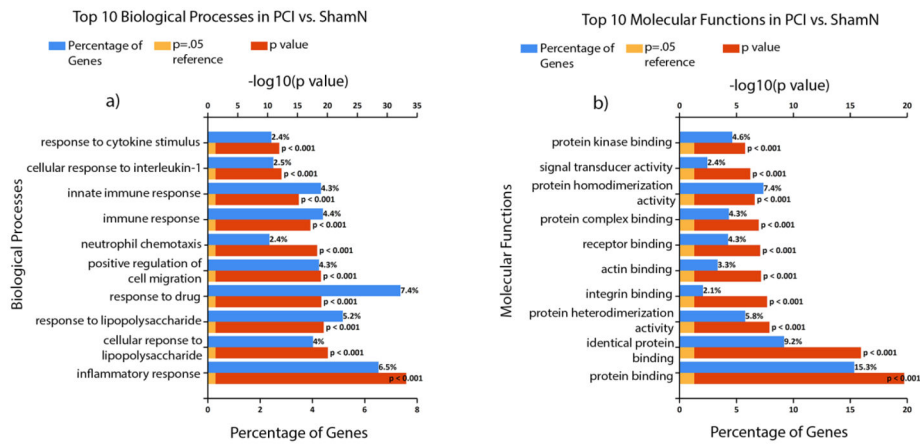
Fig. 4.

Functional analysis figures were generated with FunRich 3.0 [16] and Gene Ontology (GO) Norway rat (Taxon ID: 10116) database [17, 18]. Shown are the top 10 biological processes (**a**) and molecular functions (**b**) for PCI *vs* ShamN arranged according to increasing P (or decreasing $\log_{10}$(P value)). Percentage of differentially expressed genes belonging to each process is shown as blue bars. $\log_{10}$(P =0.05) is shown as a reference.
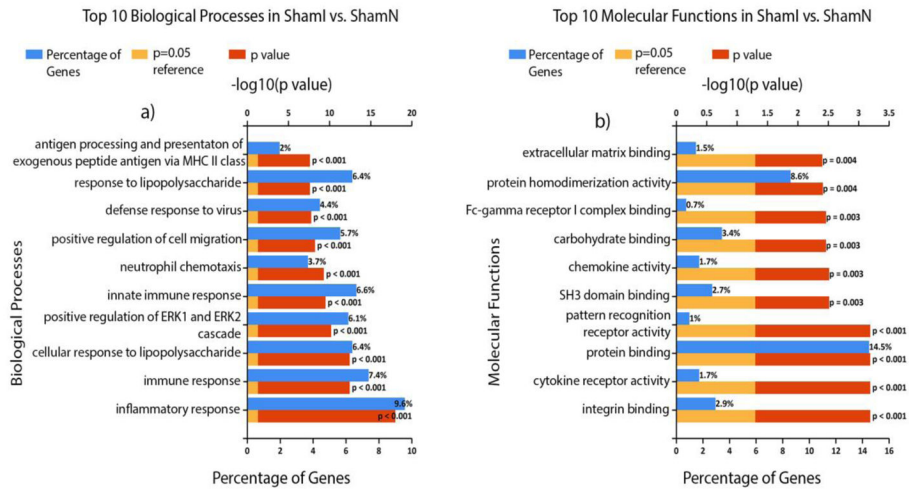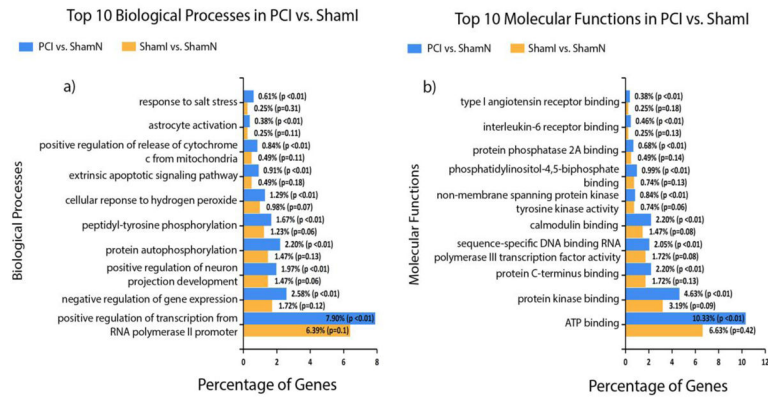
Fig. 5.
Functional analysis figures were generated with FunRich 3.0 [16] and Gene Ontology (GO) Norway rat (Taxon ID: 10116) database [17, 18]. Shown are the top 10 biological processes (**a**) and molecular functions (**b**) for ShamI *vs* ShamN, arranged according to increasing P (or decreasing $-\log_{10}$(P value)). Percentage of differentially expressed genes belonging to each process is shown as blue bars. $-\log_{10}$(P =0.05) is shown as a reference.

Fig. 6.

Top 10 biological processes (**a**) and molecular functions (**b**) "uniquely" affecting PCI *vs* ShamN, i.e. biological processes and functions with P ≤ 0.05 in PCI *vs* ShamN and P > 0.05 in ShamI *vs* ShamN. Figures were generated with FunRich 3.0[16] and Gene Ontology (GO) Norway rat (Taxon ID: 10116) database [17, 18].Percentage of DEGs belonging to a particular process/function is shown in blue bars (PCI) and yellow bars (ShamI).
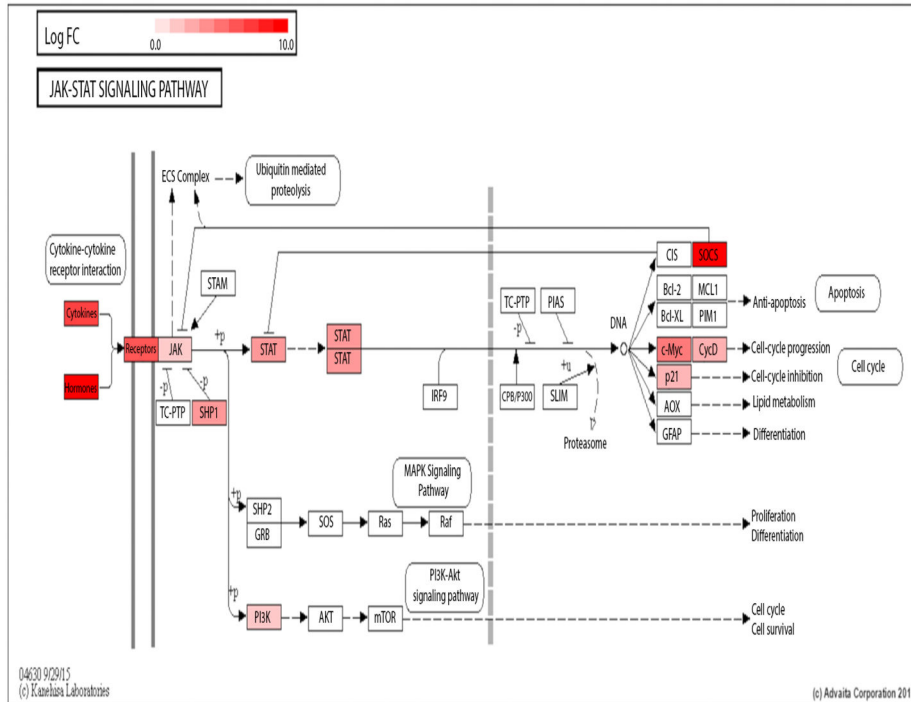
Fig. 7.
Jak-STAT KEGG pathway diagram for PCI *vs* ShamN and ShamI *vs* ShamN respectively. Diagrams were downloaded from iPathwayGuide's pathways feature [19]. Significantly affected genes between conditions are colored and the intensity of the color reveals the magnitude of the fold change of a given gene (genes in red indicate up-regulation; genes in blue indicate down-regulation). Only the genes with an absolute value of log₂(fold change) 2 and Q 0.05 were considered significant.
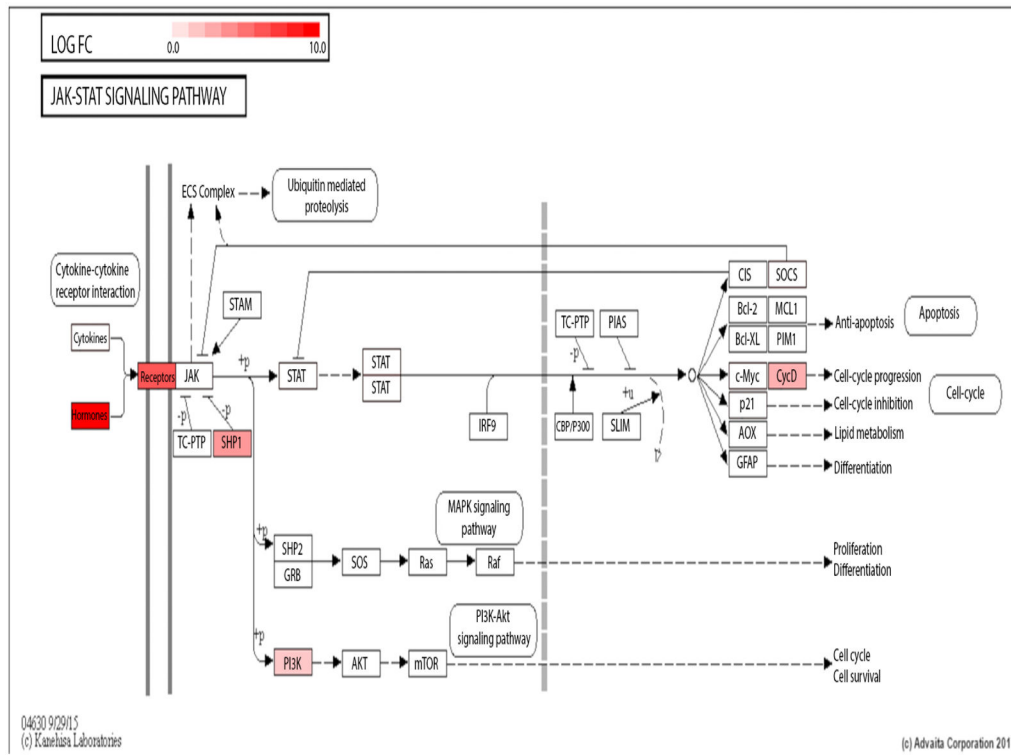
Fig. 8.

Jak-STAT KEGG pathway diagram for PCI *vs* ShamN and ShamI *vs* ShamN respectively. Diagrams were downloaded from iPathwayGuide's pathways feature [19]. Significantly affected genes between conditions are colored and the intensity of the color reveals the magnitude of the fold change of a given gene (genes in red indicate up-regulation; genes in blue indicate down-regulation). Only the genes with an absolute value of log_2(fold change) 2 and Q 0.05 were considered significant.

Table 1

Top 20 differentially expressed genes according to descending Q values for PCI vs. ShamN and ShamI vs. ShamN respectively. The values were obtained as a result of the differential expression pairwise tests in edgeR. Table was generated using by edgeR_3.12.1.

Top 20 Genes for ShamI vs. ShamN				Top 20 Genes for PCI vs. ShamN			
ID	Gene Name	logFC	Q value	ID	Gene Name	logFC	Q value
Pde6h	phosphodiesterase 6H	−2.279	1.31E-10	Spp1	secreted phosphoprotein 1	4.780	1.92E-16
Nckap 11	NCK associated protein 1 like	3.563	1.84E-07	Mrpl43	mitochondrial ribosomal protein L43	7.822	2.32E-15
Rassf4	Ras association domain family member 4	1.817	1.02E-06	Top2a	topoisomerase (DNA) II alpha	4.359	1.03E-13
Txnip	thioredoxin interacting protein	2.312	1.40E-06	Alcam	activated leukocyte cell adhesion molecule	2.529	1.03E-13
RT1-Da	RT1 class II, locus Da	4.833	4.25E-06	Gpnmb	glycoprotein nmb	4.443	1.36E-12
Mpeg1	macrophage expressed 1	3.683	5.02E-06	Mki67	marker of proliferation Ki-67	4.818	3.92E-12
Tifab	TIFA inhibitor	4.009	7.02E-06	RT1-DMb	RT1 class II, locus DMb	4.524	4.68E-12
Arr3	arrestin 3	−2.146	1.58E-05	Cenpf	centromere protein F	4.224	6.16E-11
Fcgr2b	Fc fragment of IgG, low affinity IIb, receptor	10.693	1.58E-05	Rassf4	Ras association domain family member 4	2.172	1.66E-10
Bin2	bridging integrator 2	4.106	2.62E-05	Alox5ap	arachidonate 5-lipoxygenase activating protein	3.042	1.09E-09
Mlf1	myeloid leukemia factor 1	2.064	2.62E-05	Ctsz	cathepsin Z	4.345	3.04E-09
Ctss	cathepsin S	2.042	2.95E-05	Vim	vimentin	2.490	3.28E-09
Laptm5	lysosomal protein transmembrane 5	4.315	3.81E-05	Pdpn	podoplanin	2.526	2.68E-08
Csf1r	colony stimulating factor 1 receptor	3.103	3.84E-05	Ptafr	platelet-activating factor receptor	5.885	2.69E-08
Gadd45g	growth arrest and DNA-damage-inducible, gamma	1.882	3.84E-05	Lmna	lamin A/C	2.529	3.31E-08
Clec4a1	C-type lectin domain family 4, member A1	8.195	5.45E-05	Cd44	CD44 molecule (Indian blood group)	4.005	3.70E-08
Aif1	allograft inflammatory factor 1	3.743	5.45E-05	Mlf1	myeloid leukemia factor 1	2.165	3.70E-08
Mt2A	metallothionein 2A	2.500	6.77E-05	Lipa	lipase A, lysosomal acid type	1.702	3.70E-08
Ncf1	neutrophil cytosolic factor 1	6.501	7.23E-05	Ncf1	neutrophil cytosolic factor 1	7.056	5.80E-08
Apobec1	apolipoprotein B mRNA editing enzyme catalytic subunit 1	4.109	0.000115	Arpc1b	actin related protein 2/3 complex, subunit 1B	3.784	5.92E-08

Table 2

KEGG pathways unique to PCI vs. ShamN group. The list was compiled by comparing significantly affected pathways in PCI vs. ShamN to ShamI vs. ShamN and keeping only the ones unique for the former. No pathways were unique for the latter. The list of affected pathways was generated by iPathwayGuide. Pathways with FDR value .05 in PCI vs. ShamN and Q value > .05 in ShamI vs. ShamN are shown. Biologically related pathways are bolded.

PCI vs. ShamN Unique Pathways	
Pathway name	**p-value**
MAPK signaling pathway	**1.05E-06**
Regulation of actin cytoskeleton	2.66E-05
Apoptosis	**6.87E-05**
Measles	7.73E-05
Jak-STAT signaling pathway	**8.69E-05**
Focal adhesion	1.75E-04
Hepatitis B	1.88E-04
PI3K-Akt signaling pathway	**2.48E-04**
Non-alcoholic fatty liver disease (NAFLD)	5.06E-04
Insulin resistance	8.77E-04
Adipocytokine signaling pathway	9.10E-04
Pathways in cancer *	9.84E-04
Cytosolic DNA-sensing pathway	0.002
Amyotrophic lateral sclerosis (ALS)	0.003
HIF-1 signaling pathway	**0.005**
Viral carcinogenesis	0.008
Epstein-Barr virus infection	0.008
Rap1 signaling pathway	0.008
T cell receptor signaling pathway	0.01
p53 signaling pathway	**0.013**
Platelet activation	0.017
MicroRNAs in cancer *	0.019
Adherens junction *	0.029
Small cell lung cancer	0.034
RIG-I-like receptor signaling pathway	0.047
Arginine and proline metabolism *	0.047
Bladder cancer	0.048
Cell cycle	**0.049**

Author Manuscript

Author Manuscript

Author Manuscript

Author Manuscript

Table 3

Uniquely affected genes in Jak-STAT KEGG pathway for PCI vs. ShamN along with their associated FDR values and fold changes in both comparison groups. Genes are displayed along with their respective log$_2$FC ratio, p value and Q value.

Jak-Stat Pathway

ID	Gene Name	PCI vs. SHAMN: logFC	PCI vs. SHAMN: PValue	PCI vs. SHAMN: QValue	SHAMI vs. SHAMN: logFC	SHAMI vs. SHAMN: PValue	SHAMI vs. SHAMN: QValue
Cytokines	Csf2	7.415	0.001	0.014	4.590	0.147	0.658
	Il6	7.415	0.001	0.015	6.131	0.049	0.410
	Il11	5.902	0.003	0.036	4.445	0.107	0.592
	Il23a	4.362	0.000	0.009	1.366	0.362	0.868
Receptors	Csf2rb	6.545	0.002	0.026	4.496	0.092	0.560
	Csf3r	5.245	0.000	0.002	4.638	0.004	0.097
	Il13ra2	4.955	0.000	0.005	3.518	0.036	0.349
	Il2rg	4.643	0.001	0.017	4.282	0.004	0.090
	Csf2ra	2.544	0.002	0.022	2.225	0.009	0.164
	Il6r	2.475	0.000	0.000	1.830	0.013	0.196
	Ifngr2	2.142	0.000	0.002	1.729	0.001	0.025
JAK	Jak2	2.079	0.000	0.008	1.140	0.071	0.501
STAT	Stat6	3.999	0.003	0.034	1.881	0.323	0.851
c-Myc	Myc	5.167	0.000	0.001	3.766	0.007	0.142
p21	Cdkn1a	2.876	0.000	0.008	1.663	0.034	0.339
SOCS	Socs3	7.776	0.001	0.011	6.127	0.023	0.276